Optical two-beam traps in microfluidic systems

Berg-Sørensen, Kirstine

Published in:
Japanese Journal of Applied Physics

Link to article, DOI:
10.7567/JJAP.55.08RA01

Publication date:
2016

Document Version
Peer reviewed version

Optical two-beam traps in microfluidic systems

Kirstine Berg-Sørensen*

Department of Physics, Technical University of Denmark, 2800 Kgs Lyngby, Denmark

An attractive solution for optical trapping and stretching by means of two counterpropagating laser beams is to embed waveguides or optical fibers in a microfluidic system. The microfluidic system can be constructed in different materials, ranging from soft polymers that may easily be cast in a rapid prototyping manner, to hard polymers that could even be produced by injection moulding, or to silica in which waveguides may either be written directly, or with grooves for optical fibers. Here, we review different solutions to the system and also show results obtained in a polymer chip with DUV written waveguides and in an injection molded polymer chip with grooves for optical fibers.

1. Introduction

Since Arthur Ashkin first manipulated live objects,[1)] optical trapping and manipulation by single-beam traps, aka optical tweezers has evolved from a method being investigated in research labs, to a commercially available tool,[2)] at present even with commercial equipment of a quality comparable to that in the most advanced labs available.[3,4)] But Ashkins original work involved also counter-propagating laser beams, a possibly more intuitive suggestion for trapping by means of light. Such counter-propagating laser beam traps were later developed into the so-called optical stretcher[5)] which is conveniently implemented in a microfluidic system.[6–8)] The optical stretcher is a valuable tool for investigation of elasticity of cells, and has been suggested as a tool for diagnosis.[9)]

For the optical stretcher to work in a microfluidic setting, the counter-propagating beams should be well aligned.[10)] If the counter-propagating beams are delivered by optical fibers, this implies that opposing fiber grooves should be well aligned. With an SU-8 structure modified by photo-lithography for fiber grooves and for the positioning of a square capillary for the microfluidic channel, as in reference 6, alignment is ensured, whereas with optical fibers positioned in a PDMS structure, alignment is possible but requires a somewhat complicated procedure.[11)] Another option is to form waveguides in the material of the microfluidic chip, e.g. by femtosecond direct laser writing in glass

*E-mail address: kirstine.berg-sorensen@fysik.dtu.dk

chips.[8,12)]

A recurrent problem to consider with a microfluidic stretcher setup is also how to ensure that the cells that one wishes to trap and stretch flow through the counter-propagating laser beams at the correct height whereby they are subject to the optical forces. One may rely on the balance between hydrodynamic lift and gravity to position the cells, but since this balance depends in a complex manner on the interplay between density, mass and size of the cells, different flow conditions are required for each new cell type. Another solution is to apply sound waves, also known as acoustophoresis,[13)] to position the cells at the correct height. For the density and size of most cells, acoustophoresis dominates by far over the effects of gravity.

This paper reviews our efforts to construct optical stretchers in a microfluidic chip with a view to solving the problem of cells flowing at the wrong height, and at the same time, with a view to construct the microfluidic system in a non-expensive polymer system and if possible, by methods allowing for mass production. The sections below therefore describes first a glass-polymer microfluidic system in which acoustopheretic prefocusing was demonstrated, followed by a section on a pure silica microfluidic system in which the acoustophoretic prefocusing was demonstrated to work very well. The following two sections describe all-polymer microfluidic systems, produced by hot embossing and post-processing by UV light in the former case, and by injection molding and postmounting of optical fibers for the latter. Finally, we conclude and suggest roads for future development.

2. Combined polymer-glass system for prefocusing by acoustophoresis

In a quest for the construction of a relatively cheap microfluidic system, without the need for any cleanroom processing, a design based on cast molding in PDMS was investigated.[14)] In addition to the liquid channel being defined in PDMS and fibers being positioned in PDMS, the system sought to investigate improvements in the optical manipulation capability when cells were pre-positioned by an acoustic field. The acoustic field acts to lift and keep the cells at the height of interception with the light emanating from single mode optical fibers.

The efficiency of acoustophoresis depends on the acoustic properties of the material in question, and important material parameters are listed in Table I. One observes from Table I a design challenge for the construction of an efficient acoustic system with both PDMS and water: the sound speed and the acoustic impedance in PDMS is even lower

Table I. For acoustophoresis, different material parameters must be considered: The density ρ_0 (at 20° C), the speed of sound, c_a[15], and the acoustic impedance. Values were found in reference 16 or obtained from the manufacturer (for soda-lime glass and piezo-ceramic).

	ρ_0 (kg/m^3)	c_a (m/s)	$Z \equiv \rho_0 c_a$ (kg/(m^2 s))
Air	1.16	343.4	$3.98 \cdot 10^2$
Water	998	1483	$1.48 \cdot 10^6$
Soda-lime glass	2440	5804	$1.42 \cdot 10^7$
PDMS	965	1076	$1.04 \cdot 10^6$
Piezoceramic	8000	4000	$3.2 \cdot 10^7$

than in water, and it is expected that a large fraction of the acoustic energy is lost in the polymer material and thus not available for the acoustic manipulation of cells in the water channel. We therefore reduced the amount of PDMS as much as possible but also observed, by trial and error, that with the overall dimensions of the system that we had chosen, the water channel should be at least three times as wide as high. For the same reason, we chose to have both lid and bottom of the water channel in a hard material, with good acoustic transmission. Since the system should be accessible by optical microscopy, in our case by an inverted microscope, a transparent material is necessary and (soda-lime) glass was chosen for both lid and bottom. This has the added benefit that a tight bonding between the PDMS layer and glass lid and bottom is possible by means of plasma bonding in an oxygen plasma.

Acoustic excitation is easy to induce by means of a piezo-ceramic disk with resonance frequency close to that of the microfluidic system. We further observe that the sound speed in soda-lime glass is close to four times that in water, and optimal transfer of acoustic energy from piezo-ceramic to the water channel was obtained by choosing the thickness of the bottom layer in glass, in contact with the piezo-ceramic, such that in resonance, half a sound wave in glass, then half a sound wave in water and finally a quarter wave - thereby well reflected at the interface between glass and air - was induced by the piezo-ceramic. The geometry is illustrated in Fig. 1.

The acoustophoretic prefocusing was demonstrated to work and position both polystyrene beads, red blood cells and even soft objects like Giant Unilamellar Vesicles (GUVs) in the middle of the channel, at the same height within the liquid channel as the core of the optical fibers in a well-assembled microfluidic chip system.[14] The material required to produce one chip is inexpensive - we even used standard white

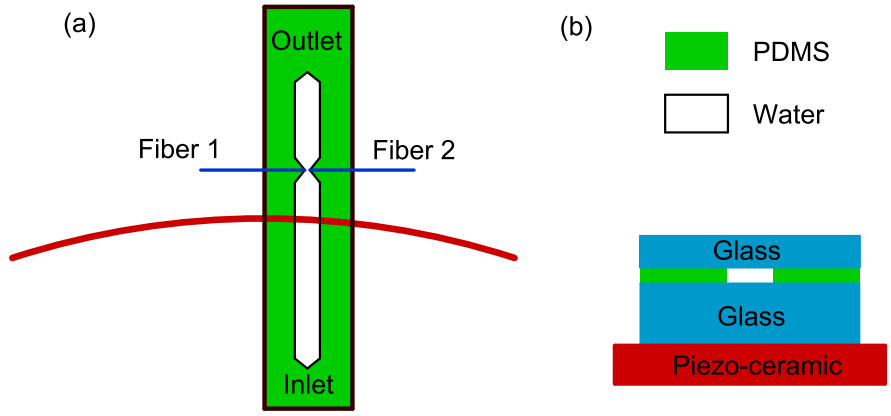

Fig. 1. (Color online) Sketch of the preferred microfluidic chip design of the glass-PDMS-glass sandwich with optical fibers, and mounted on a piezo-ceramic disk with resonance frequency of 1.5 MHz. Part a) shows the system seen from the top, the red arc indicates the position of the piezo-ceramic disk underneath the microfluidic chip. Blue lines indicate the two optical fibers, whereas green shading indicates the microfluidic channel molded in PDMS. The odd-shaped liquid channel includes both wide parts, to ensure that acoustic prefocusing works, and a narrow part ensuring a short (approximately 100μm) distance between fiber tips, to have good optical trapping. The overall dimensions of the PDMS part is 8mm x 32mm, whereas the corresponding glass parts for top and bottom are 7mm x 32mm. The small difference in width is chosen to avoid that the fiber is bonded to the glass top or bottom during plasma bonding. Part b) shows the chip seen from one of the short ends, illustrating the 2 mm thick glass bottom part, the 0.5 mm thick PDMS part, and the 1 mm thick glass top part. Underneath the glass-PDMS-glass sandwich, the piezo-ceramic is indicated by red shading. The liquid channel within the PDMS part has a corresponding height of $h = 500\mu$m, and a simple one dimensional estimate of the standing sound wave resonance frequency, $f = c_a/(2h)$, corresponds therefore to 1.5 MHz.

glass microscope slides that were cut into pieces of the requested size of 7mm x 32mm. Nevertheless, with the chip assembly being manual, often the fiber positioning in the soft PDMS lacked precision in the alignment, resulting in the request of a new chip being made. Although this alignment problem can be circumvented, as demonstrated in reference 11, we chose to rather investigate other design options.

3. All-glass chip with prefocusing by acoustophoresis

With a microfluidic chip constructed entirely in a hard material like glass (cf. Table I), acoustophoretic prefocusing works even better. Thus, with an all-glass chip, less electrical energy is required to drive the piezo-ceramic crystal, and consequently, less heating in the system is expected. Also, there is less need to carefully tune the thickness

Table II. The cross-sectional dimensions of the two all-glass chips investigated, and the expected resonance frequencies as evaluated by the Helmholtz wave equation (see reference 19), $f_{n_x,n_y} = c_a/2\sqrt{(n_x/w)^2 + (n_y/h)^2}$

Chip	Width, w (μm)	Height, h (μm)	$f_{(1,0)}$ (MHz)	$f_{(0,1)}$ (MHz)	$f_{(1,2)}$ (MHz)
Rectangular	100	240	7.5	3.1	8.1
Square	150	150	5.0	5.0	

of the bottom and top layer of glass surrounding the water. In an all-glass chip, optical fields for trapping are conveniently delivered by waveguides constructed by direct femto-second laser writing[8,12,17] in the glass. In reference 17, two all-glass microfluidic chips were constructed and tested, with a rectangular and a square cross-section of the fluidic channel, both with their benefits: With the square cross-section, the same piezo-ceramic can excite both the vertical (y) and the horisontal (x) standing wave, resulting in cells being not only at the correct height for the optical stretching, but also right in the middle between the ends of the two waveguides. With the rectangular cross-section, two different piezo-crystals can be coupled to the chip at once, enabling experimental assays that can benefit from this addiitonal degree of freedom. The overall chip design is illustrated in Fig. 2 while dimensions and expected resonance frequencies are stated in Table II. In a different chip with waveguides prepared in a similar manner, the propagation losses for 543 nm laser light were measured to be 0.9 dB/cm.[18] With the addition of acoustic prefocusing, a doubling of the trapping efficiency was demonstrated, and in addition, it was shown that the acoustic prefocusing had no discernible effect on the optical deformability of either red blood cells or on mouse fibroblast cells.

4. Polymer chip with DUV written waveguides

Despite the clear advantages of the all-glass system described in the previous section, the glass chip is relatively expensive to buy and the modifications with femto-second laser writing requires availability of both quite advanced equipment and time in the lab. Therefore, once produced, a microfluidic chip must be safe-guarded, kept clean and re-used for a long period of time. Microfluidic chips produced in a less expensive material like a polymer material, and requiring less time-consuming handling during the production procedure, are therefore worth looking for. Fortunately, also polymeric materials may have changes in the optical properties induced by treatment with light: treatment with deep UV light (λ of 325 nm or 365 nm) of ordinary polymethylmethacry-

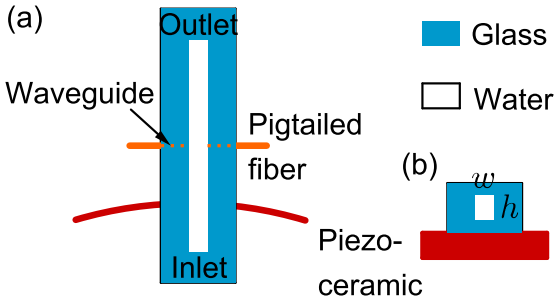

Fig. 2. (Color online) Overview of the design of the all-glass chip with waveguides; light is coupled to the waveguides through pigtailed optical fibers and the entire glass chip is mounted on a piezo-ceramic disk with resonance frequency matching the particular values for the width w and the height h of the liquid channel. Part a) shows the system seen from the top, the red arc indicates the position of the piezo-ceramic disk underneath the microfluidic chip. The glass part is light blue, with the liquid channel (denoted "Water"). Part b) shows the chip seen from one of the short ends. Underneath the glass chip, the piezo-ceramic is indicated by red shading. The liquid channel has height h, and width w.

late (PMMA, also known as plexiglass) induces changes in the refractive index,[20] and was applied for a pre-prototype of an optical stretcher microfluidic chip in reference 21. DUV treatment is a relatively simple postprocessing step, just requiring a photo-mask and DUV light available. In our case, DUV treatment followed hot embossing of a microfluidic channel, but one could equally well carry out the DUV treatment step as a post-processing step to add functionality to an injection molded polymer system.

With this system, and an image analysis procedure that allows to track several particles that were subject to both flow and optically induced forces, the functionality of the DUV induced waveguides were demonstrated as illustrated in Fig. 3, and the optically induced force determined. The loss in the waveguides was measured by writing curved waveguides of different length, coupling light into the waveguide and measuring the relative loss in transmitted optical power. Based on these measurements, the loss was found to be 0.66 ± 0.13 dB/mm for laser light of a wavelength of λ=808 nm. The loss is higher than in the femto-second written waveguides in fused silica but comparable to losses reported for other UV induced waveguides.[22,23]

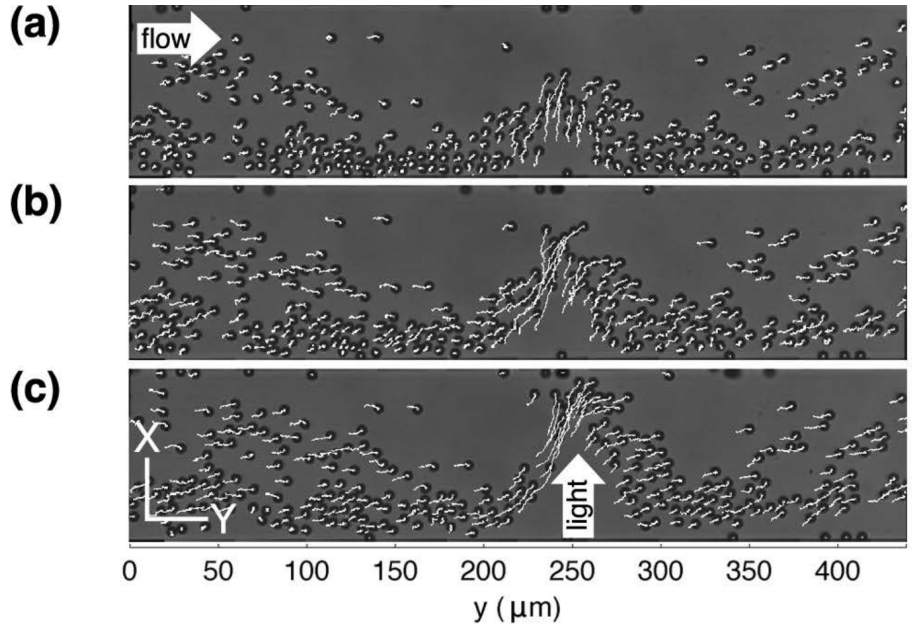

Fig. 3. Sequence of three images showing particles in flow being traced by a multi-bead particle tracing algorithm. The image sequence with bead tracing illustrates how the particles respond to the optical force from 808 nm light coupled into the DUV induced waveguide. Part a) shows the initial situation for particles in flow traced over a short time, the position of the light coupled into the waveguide is at $y = 250$ μm. Part b) and part c) illustrates the bead positions and bead position traces at two later points in time. Modified from reference 21.

5. Injection molded polymer chip with post-processing by insertion of optical fibers

One issue with microfluidic chips with DUV or femto-second written waveguides is the loss of optical power. The design described in section 2 did not suffer from loss of optical power because the commercially available optical fibers used for light delivery are basically lossfree. A microfluidic chip in a low-cost material and produced by production grade technology, with a more well-defined alignment of the optical fibers than that seen in the glass-PDMS-glass sandwich chip investigated earlier, was therefore investigated as well.[24] The chip was produced in hard Cyclic Olefin Copolymer (CoC) TOPAS 5013 by injection molding based on a Nickel shim with a multi-layer structure. This allowed for the construction of a polymer chip with square grooves of nominally 125 μm depth and width, to accommodate stripped 125 μm diameter optical fibers. The fiber grooves were positioned perpendicular to a square groove of nominally 100 μm depth and width for the microfluidic channel, as illustrated in the right inset of Fig. 4. In addition, the chip was constructed with three inlets, to allow for laminar focusing of cells or particles

that were injected in the middle channel. Fluidic inlets and outlets were easily connected to liquid reservoirs via LUER fittings molded at the top side of the microfluidic chip. Single mode optical fibers were mounted in the chip in a postprocessing step, following which the system was closed through pressure bonding of a polyolefin film. Fibers were measured to have a lateral alignment accuracy of 2.7 ± 1.8 μm.

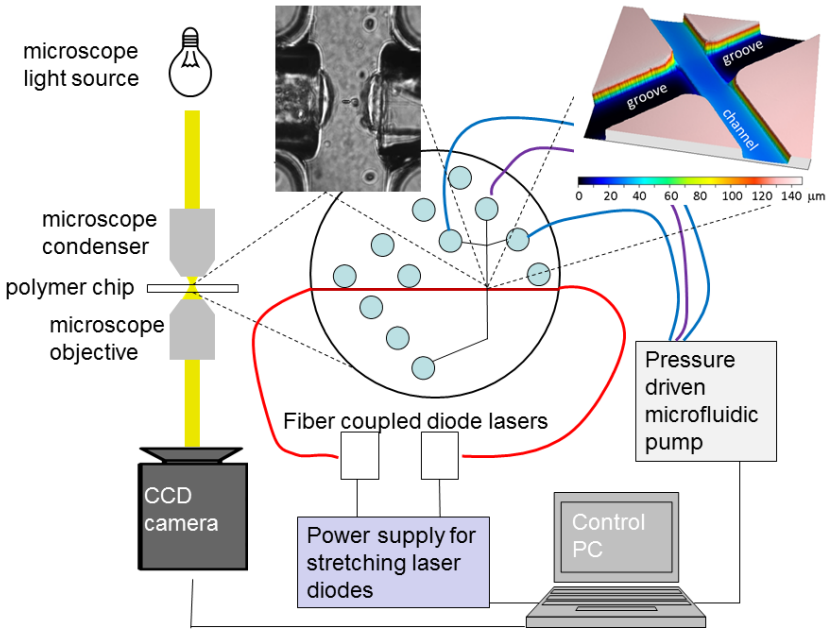

Fig. 4. (Color online) Sketch of the experimental setup with the polymer microfluidic chip. Light from two fiber-coupled 1064 nm lasers is delivered through single mode optical fibers that are inserted in the injection molded polymer chip in a postprocessing step. The flow is controlled by a pressure-controlled microfluidic pump, and images recorded by a CCD camera mounted on the optical microscope. Both lasers, pump and camera are controlled by computer via a custom-written LabView interface. Insets show (right) the profile of the polymer chip before insertion of optical fibers, as measured in a confocal microscope, and (left) an optically trapped and stretched red blood cell; the scale is given by the fiber diameter of 125 μm. Modified from reference 24.

The ease of handling of the system was demonstrated by the fact that the chip was originally developed for a summer school in which students with no prior training could assemble the chip and perform optical stretching experiments of red blood cells within two-three days of practical work in the laboratory.[25] The full setup with the polymer microfluidic chip positioned on the stage of an inverted microscope, with computer controlled pressure driven pump, laser coupled diode lasers and CCD camera is illustrated in Fig. 4, in which the left inset also shows a red blood cell being trapped and slightly

stretched.

6. Discussion and conclusions

Optical stretching is a valuable tool to investigate mechanical properties of cells, and has been used in several different cases including for investigations of cancerous versus healthy cells[9] or for investigations of stem cell fate,[26] and the technique may be coupled to subsequent cell sorting as based on the mechanical characteristics.[27] As illustrated by the examples detailed in this review, experimental setups relying on production ready chip fabrication are well within reach. One of the important advantages of the optical stretcher as a tool to determine mechanical properties of single cells is the fact that it is slow enough for choices to be made that enable subsequent investigations of cells that have been chosen as particularly interesting. So far, research applying optical stretchers has been very much concentrated on cancer cells, but we imagine other cell types as interesting too, and have preliminary results indicating differences between red blood cells from healthy donors and red blood cells from patients with e.g. cytoskeletal defects.

The fact that optical stretcher experiments are slow enough for choices to be made during an experiment with respect to subsequent investigations of particular cells is also a disadvantage of the technique: Even with unprecedented, but currently possible, improvements in fast image analysis, the method at present relies on careful fluidic handling requesting human intervention and it is hard to imagine it being developed into a true high-throughput technique. In contrast, recent years have demonstrated how high throughput may be achieved when fluidic shear forces are applied to investigate cellular mechanical properties through what has been coined the deformability of the cell.[28–30] This is a very interesting development, in particular so if one could imagine combining the high throughput of the flow-based techniques with computer vision and optical manipulation to also be able to sort and subsequently investigate a subset of single cells in more detail. This may be relevant in cases where a small subpopulation of cells carry the interesting features. As an important example, we note that current research in causes of cancer seems to indicate that cancer cells form a heterogeneous or mixed population[31,32] potentially including differences in mechanical properties. Biopsies from patients may therefore form such a mixed population and it would be highly relevant to identify the most aggressive, or the cells with the highest potential for metastasis.

Acknowledgment

The experimental work reviewed in detail in this manuscript relied on support from the Carlsberg Foundation, from the COST action MP1205 and from the Danish Council for Strategic Research through the PolyNano project. The author is endebted to efforts from students and postdocs who have been working in her laboratory over the past five years, doing smaller and larger projects, ranging from BSc theses to the work of trained postdocs.

References

1) A Ashkin and J Dziedzic. Optical trapping and manipulation of viruses and bacteria. *Science*, 235:1517–1520, 1987.
2) Thorlabs online catalogue; www.thorlabs.de.
3) LUMICKS; www.lumicks.com; C-Trap^{TM}.
4) JPK instruments; www.jpk.com; NanoTracker^{TM}.
5) Guck J, Ananthakrishnan R, Mahmood H, Moon TJ, Cunningham CC, and Käs J. The optical stretcher: A novel laser tool to micromanipulate cells. *Biophys. J.*, 81(2):767 – 784, 2001.
6) Bryan Lincoln, Stefan Schinkinger, Kort Travis, Falk Wottawah, Susanne Ebert, Frank Sauer, and Jochen Guck. Reconfigurable microfluidic integration of a dual-beam laser trap with biomedical applications. *Biomed. Microdevices*, 2007.
7) F Lautenschlaeger and J R Guck. Microfluidic integration of high power dual-beam laser traps for cell mechanical measurements. In *IEEE ISOT: 2009 International Symposium on Optomechatronic Technologies*, pages 419–422, 2009.
8) N Bellini, KC Vishnubhatla, F Bragheri, L Ferrara, P Minzioni, R Ramponi, I Cristiani, and R Osellame. Femtosecond laser fabricated monolithic chip for optical trapping and stretching of single cells. *Opt. Express*, 18(5):4679–4688, 2010.
9) Torsten W Remmerbach, Falk Wottawah, Julia Dietrich, Bryan Lincoln, Christian Wittekind, and Jochen Guck. Oral cancer diagnosis by mechanical phenotyping. *Cancer. Res.*, 69:1728–1732, 2009.
10) A Constable, J Kim, J Mervis, F Zarinetchi, and M Prentiss. Demonstration of a fiber-optical light-force trap. *Opt. Lett.*, 18:1867–1869, 1993.
11) C W Lai, S K Hsiung, C L Yeh, A Chiou, and G B Lee. A cell delivery and pre-positioning system utilizing microfluidic devices for dual-beam optical trap-and-stretch. *Sens. Actuators B Chem.*, 135:388–397, 2008.
12) N Bellini, F Bragheri, I Cristiani, J Guck, R Osellame, and G Whyte. Validation and perspectives of a femtosecond laser fabricated monolithic optical stretcher. *Biomed. Opt. Express*, 3(10):2658–2668, 2012.
13) H Bruus, J Dual, J Hawkes, M Hill, T Laurell, J Nilsson, S Radel, S Sadhal, and M Wiklund. Acoustofluidics-exploiting ultrasonic standing wave forces and acoustic streaming in microfluidic systems for cell and particle manipulation

(editorial). *Lab. Chip*, 11:3579–3580, 2011.

14) M Khoury, R Barnkob, L Laub Busk, P Tidemand-Lichtenberg, H Bruus, and K Berg-Sørensen. Optical stretching on chip with acoustophoretic prefocusing. *Proc. SPIE*, 8458:84581E, 2012.
15) L Landau, E Lifshitz, A Kosevich, and L Pitaevskii. *Theory of Elasticity*. Butterworth-Heinemann, 1986.
16) D R Lide and W M Haynes. *CRC Handbook of Chemistry and Physics: A Ready-reference book of chemical and physical data*. CRC Press, 2010.
17) G Nava, F Bragheri, T Yang, P Minzioni, R Osellame, I Cristiani, and K Berg-Sørensen. All-silica microfluidic optical stretcher with acoustophoretic prefocusing. *Microfluid. Nanofluid.*, 19:837–844, 2015.
18) R Osellame, V Maselli, R M Vazquez, R Ramponi, and G Cerullo. Integration of optical waveguides and microfluidic channels both fabricated by femtosecond laser irradiation. *Appl. Phys. Lett.*, 90:231118–1 –3, 2007.
19) H Bruus. Acoustofluidics 2: perturbation theory and ultrasound resonance modes. *Lab. Chip*, 12:20–28, 2012.
20) Tomlinson WJ, Kaminow IP, Chandros EA, Fork RL, and Silfvast WT. Photoinduced refractive index increase in Poly(methylmethacrylate) and its applications. *Appl. Phys. Lett.*, 16(12):486–489, 1970.
21) M Khoury, C Vannahme, K T Sørensen, A Kristensen, and K Berg-Sørensen. Monolithic integration of DUV-induced waveguides into plastic microfluidic chip for optical manipulation. *Microelectron. Eng.*, 121:5–9, 2014.
22) Manor R, Datta A, Ahmad I, Holtz M, Gangopadhyay S, and Dallas T. Microfabrication and characterization of liquid core waveguide glass channels coated with Teflon AF. *IEEE Sens. J.*, 3(6):687–692, 2003.
23) Nimi Gopalakrishnan, Kaushal S. Sagar, Mads Brokner Christiansen, Martin E. Vigild, Sokol Ndoni, and Anders Kristensen. UV patterned nanoporous solid-liquid core waveguides. *Opt. Express*, 18(12):12903–12908, 2010.
24) M Matteucci, M Triches, G Nava, A Kristensen, M R Pollard, K Berg-Sørensen, and R J Taboryski. Fiber-based, injection-molded optofluidic systems: Improvements in assembly and applications. *Micromachines*, 6:1971–1983, 2015.
25) PolyNano summer school; www.nanotech.dtu.dk/Uddannelse/PolyNano-summerschool.
26) J M Maloney, D Nikova, F Lautenschläger, E Clarke, R Langer, J Guck, and

K J Van Vliet. Mesenchymal stem cell mechanics from the attached to the suspended state. *Biophys. J.*, 99:2479–2487, 2010.

27) T Yang, P Paiè, G Nava, F Bragheri, R Martinez Vazquez, P Minzioni, M Veglione, M Di Tano, C Mondello, R Osellame, and I Cristiani. An integrated optofluidic device for single-cell sorting driven by mechanical properties. *Lab. Chip*, 15:1262–1266.

28) Dl R Gossetta, H T K Tse, S A Lee, Y Ying, A G Lindgren, O O Yang, J Rao, A T Clark, and D Di Carlo. Hydrodynamic stretching of single cells for large population mechanical phenotyping. *Proc. Natl. Acad. Sci. U.S.A.*, 109:7630–7635, 2012.

29) O Otto, P Rosendahl, A Mietke, S Golfier, C Herold, D Klaue, S Girardo, S Pagliara, A Ekpenyong, AJacobi, M Wobus, N Töpfner, U F Keyser, J Mansfeld, E Fischer-Friedrich, and J Guck. Real-time deformability cytometry: on-the-fly cell mechanical phenotyping. *Nat. Meth.*, 12:199–202, 2015.

30) A Mietke, O Otto, S Girardo, P Rosendahl, A Taubenberger, S Golfier, E Ulbricht, S Aland, J Guck, and E Fischer-Friedrich. Extracting cell stiffness from real-time deformability cytometry: Theory and experiment. *Biophys. J.*, 109:2023–2036, 2015.

31) C E Meacham and S J Morrison. Tumour heterogeneity and cancer cell plasticity. *Nature*, 501:328–337, 2013.

32) N S Barteneva, K Ketman, E Fasler-Kan, D Potashnikova, and I A Vorobjev. Cell sorting in cancer research - Diminishing degree of cenn heterogeneity. *Biochim. Biophys. Acta*, 1836:105–122, 2013.